

Search for TeV Gamma-Rays from Shell-Type Supernova Remnants

R.W. Lessard¹, I.H. Bond², P.J. Boyle³, S.M. Bradbury², J.H. Buckley⁴, A.M. Burdett^{2,5}, D.A. Carter-Lewis⁶, M. Catanese⁶, M.F. Cawley⁷, S. Dunlea³, M. D'Vali², D.J. Fegan³, S.J. Fegan⁵, J.P. Finley¹, J.A. Gaidos¹, T.A. Hall¹, A.M. Hillas², D. Horan³, J. Knapp², F. Krennrich⁶, S. Le Bohec⁶, C. Masterson³, J. Quinn³, H.J. Rose², F.W. Samuelson⁶, G.H. Sembroski¹, V.V. Vassiliev⁵, T.C. Weekes⁵

¹*Department of Physics, Purdue University, West Lafayette, IN 47907, USA*

²*Department of Physics, Leeds University, Leeds, LS2 9JT, UK*

³*Experimental Physics Department, University College, Belfield, Dublin 4, Ireland*

⁴*Department of Physics, Washington University, St. Louis, MO 63130, USA*

⁵*Fred Lawrence Whipple Observatory, Harvard-Smithsonian CfA, P.O. Box 97, Amado, AZ 85645-0097, USA*

⁶*Department of Physics and Astronomy, Iowa State University, Ames, IA 50011-3160, USA*

⁷*Physics Department, National University of Ireland, Maynooth, County Kildare, Ireland*

Abstract

If cosmic rays with energies < 100 TeV originate in the galaxy and are accelerated in shock waves in shell-type supernova remnants (SNRs), gamma-rays will be produced as the result of proton and electron interactions with the local interstellar medium, and by inverse Compton emission from electrons scattering soft photon fields. We report on observations of two supernova remnants with the Whipple Observatory's 10m gamma-ray telescope. No significant detections have been made and upper limits on the > 500 GeV flux are reported. Non-thermal X-ray emission detected from one of these remnants (Cassiopeia A) has been interpreted as synchrotron emission from electrons in the ambient magnetic fields. Gamma-ray emission detected from the Monoceros/Rosette Nebula region has been interpreted as evidence of cosmic-ray acceleration. We interpret our results in the context of these observations.

1 Introduction:

1.1 Hadronic Gamma-Ray Production: If SNRs are sites for cosmic-ray production, there will be interactions between the accelerated particles and the local swept-up interstellar matter. Drury, Aharonian and Volk (DAV) (1994) and Naito and Takahara (1994) have calculated the expected gamma-ray flux from secondary pion production using the model of diffusive shock acceleration. Recent observations above 100 MeV by the EGRET instrument on the *Compton Gamma-Ray Observatory* have found gamma-ray signals associated with at least three SNRs: IC 443 and gamma-Cygni (Esposito et al. 1996) and the Monoceros SNR - Rosette Nebula region (Jaffe et al. 1998). These results have been interpreted as evidence for cosmic ray acceleration using the model of DAV. A search for TeV emission from IC 433 and gamma-Cygni has already been reported by the Whipple Collaboration (Buckley et al. 1998). Here we present observations of the Monoceros SNR - Rosette Nebula region.

1.2 Leptonic Gamma-Ray Production: Gamma rays will also be produced as the result of electron bremsstrahlung and by inverse Compton emission from electrons scattering soft photon fields. Non-thermal X-ray emission, observed from several SNRs including SN 1006 (Koyama et al. 1995), and Cassiopeia A (Allen et al. 1997), has been interpreted as synchrotron radiation of high energy electrons in the ambient magnetic fields. The recent detection of SN 1006 at TeV energies by CANGAROO (Tanimori et al. 1998) has been interpreted as inverse Compton emission from these electrons scattering microwave background photons as predicted by Pohl (1996), and Mastichiadis and de Jager (1996). Here we report on observations of Cassiopeia A.

2 Observations and Analysis Techniques:

The observations reported here were taken with the Whipple Observatory's high energy gamma-ray telescope situated on Mount Hopkins in southern Arizona (Cawley et al. 1990). A camera, consisting of photomultiplier tubes (PMTs) mounted in the focal plane of the reflector, detects the Cherenkov radiation produced by gamma-ray and cosmic-ray air showers from which an image of the Cherenkov light can be reconstructed. For the observations reported here, the camera consisted of 331 PMTs (each viewing a circular field of 0.25° radius) with a total field of view of 4.8° in diameter.

We characterize each Cherenkov image using a moment analysis (Reynolds et al. 1993). The roughly elliptical shape of the image is described by the *length* and *width* parameters and its location, orientation and skewness within the field of view are given by the *distance*, α and *asymmetry* parameters, respectively. We also determine the two highest signals recorded by the PMTs (*max1*, *max2*) and the amount of light in the image (*size*). Gamma-ray events give rise to more compact shower images than background hadronic showers and are preferentially oriented and skewed towards the putative source position in the image plane. By making use of these differences, a gamma-ray signal can be extracted from the large background of hadronic showers.

2.1 Centered Point Source Observations: The traditional mode of observing potential point sources with the Whipple Observatory gamma-ray telescope is track the putative source position continuously for 28 minutes. The standard gamma-ray selection method utilized by the Whipple Collaboration is the Supercuts98. These criteria were optimized on contemporaneous Crab Nebula data to give the best sensitivity to point sources. A combination of Monte Carlo simulations and results on the Crab Nebula indicate that this analysis results in an energy threshold of ~ 500 GeV and an effective collection area of $3.0 \times 10^8 \text{cm}^2$. A detailed description of the methods used to estimate the energy threshold and collection area are given elsewhere (Mohanty et al. 1998).

To estimate the expected background, we use those events which pass all of the Supercuts98 criteria except orientation (characterized by the α parameter). We use events with α between 20° and 65° as the background region. A detailed description of this method can be found elsewhere (Catanese et al. 1998).

2.2 Extended or Offset Source Observations: When the position of the putative source is not at the center of the field of view, or is not precisely known (e.g., EGRET error circles or sources of extended emission) a different strategy must be employed. A detailed description of the technique utilized can be found elsewhere (Lessard et al. 1997).

Briefly, the method uses additional features of the images of gamma-ray induced showers to provide a unique arrival direction on an event by event basis. First, events are selected as gamma-ray like based on their compactness. The determination of the arrival direction of the candidate gamma-ray events is then accomplished by making use of the orientation, elongation and asymmetry of the image. Monte Carlo studies have shown that gamma-ray images are a) aligned towards their source position on the sky b) elongated in proportion to their impact parameter on the ground and c) have a cometary shape with their light distribution skewed towards their point of origin in the image plane. Results on the Crab Nebula indicate that the angular resolution function for the telescope using this technique is a Gaussian with a standard deviation of 0.12° (Lessard et al. 1997). The efficacy of the method is demonstrated by observations in which the center of the field of view is offset from the Crab Nebula position. A combination of Monte Carlo simulations and results on the Crab Nebula indicate that this analysis results in an energy threshold of ~ 500 GeV and an effective collection area of $3.0 \times 10^8 \text{cm}^2$ for a source at the center of the field of view and is reduced for offset sources.

The analysis of data from a point source, offset from the center of the field of view, involves counting the number of events whose arrival directions fall within a circular aperture centered on the putative source location. The radius of the circular aperture has been determined by optimization of data taken on the Crab Nebula and is found to be 0.32° . The analysis of data from an extended region involves counting the number of events whose arrival directions fall within a circular aperture which encompasses the emission region plus twice the width of the angular resolution function to account for smearing of the image.

Table 1: Flux upper limits for the SNR Cassiopeia A and the Monoceros SNR - Rosette Nebula region. The result for Cassiopeia A was obtained by utilizing the method described in section 2.1, while the results for the Monoceros SNR - Rosette Nebula region were obtained utilizing the analysis method described in section 2.2.

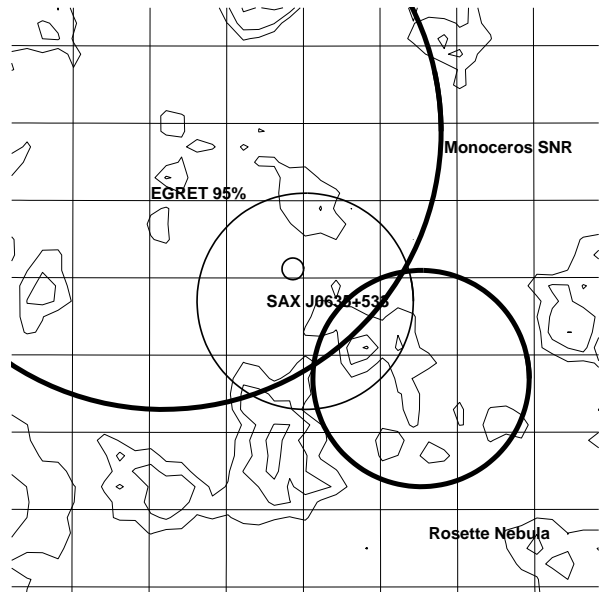
Source Name	α, δ (J2000)	aperture (degrees)	$F(E > 500 \text{ GeV}) \times 10^{-11} \text{ cm}^2 \text{ s}^{-1}$
CAS-A	23:23:23,58:48:11	-	<0.66
Monoceros SNR - Rosette	06:35:00,05:21:00 J0635+0533	1.00 0.32	<4.80 <1.41

In both cases the background is obtained from an equal amount of time tracking a position offset by 30 minutes in right ascension but with the same declination as the on source observation.

3 Results:

4.1 Monoceros SNR - Rosette Nebula Region:

The Monoceros SNR - Rosette Nebula region was observed for a total of 13.1 hours during the period November 1998 to February 1999. The contours depicted in Figure 2 show the statistical significance of the excess events recorded within the camera's sensitive field of view. The large thick circle depicts the position and extent of the Monoceros SNR while the smaller thick circle depicts the position and extent of the Rosette Nebula (a star forming region). The large thin circle depicts the EGRET 95% confidence error circle and the small circle depicts the position of a hard spectrum X-ray point source, J0635+0533, recently detected by the Italian-Dutch satellite BeppoSAX (Kaaret et al. 1999). No significant excess is detected. In the absence of a detection we have calculated flux upper limits based on two assumptions. First, that the emission detected by EGRET arises from the X-ray point source J0635+0533. In this case we have calculated a flux upper limit using the



0.08° which is smaller than the angular resolution of the photon arrival direction reconstruction. Hence, we have applied the centered point source method as given discussed above. No emission is detected and the 99.9% confidence level upper limit is given in Table 1.

4 Discussion:

4.1 The Monoceros SNR - Rosette Nebula

Region: The Whipple upper limits and EGRET data (Jaffe et al. 1998) for the Monoceros SNR - Rosette Nebula region are shown in Figure 3. Under the assumption that the emission detected by EGRET is due to cosmic-ray interactions we normalize the model of DAV to the EGRET > 100 MeV flux. The shaded area depicts a range of the spectral index of the proton population used in the model (2.1 - 2.3). As shown, the upper limits reported here require the source spectrum to be steeper than $E^{-2.2}$ or require a spectral break. Another possible explanation for the results is that the EGRET flux is produced not by cosmic-ray interactions but rather by the X-ray point source J0635+0533 which has been associated with a Be binary system (Kaaret 1999). In this case, the upper limit reported here lies two

